

# CANCELING STATIONARY INTERFERENCE SIGNALS EXPLOITING SECONDARY DATA

*Johan Swärd and Andreas Jakobsson*

Dept. of Mathematical Statistics, Lund University, Sweden

## ABSTRACT

In this paper, we propose a novel interference cancellation method that exploits secondary data to estimate stationary interference components present in both the primary and the secondary data sets, thereby allowing for the removal of such interference from the data sets, even when these components share frequencies with the signal of interest. The algorithm estimates the present interference components one frequency at a time, thus enabling for a computationally efficient algorithm, that require only a limited amount of secondary data. Numerical examples using both simulated and measured data show that the proposed methods offers a notable gain in performance as compared to other interference cancellation methods.

*Index Terms*— Interference cancellation, Radio frequency spectroscopy, Signal of interest-free data.

## 1. INTRODUCTION

Interference cancellation is an important topic in a variety of different applications, such as in radar [1,2], wireless communication [3,4], spectroscopy [5,6], cognitive radio [7], and underwater acoustics [8]. If inadequately treated, the presence of strong interference signals may easily corrupt the measurement, making detection or identification performance unreliable. Various forms of hardware based interference suppression, including shielding the measurements properly, if feasible, are often of notable importance, although further processing is typically required. A variety of signal processing techniques have been suggested for dealing with interference, many of which exploits various forms of secondary data that does not contain the signal of interest (SOI). Typical solutions include, e.g., projecting the measured signal onto the null-space of the interference [5, 9–11], using oblique projections [12], or forming adaptive detectors using generalized likelihood ratio tests [13]. A common problem with these form of techniques occurs when the SOI and the interference signal have overlapping frequencies, in which case a projection onto the interferences null-space might cancel both the interference and the SOI. Another typical problem with this

kind of methods is the need for large amounts of secondary data, which often may need to be noticeably larger than the primary data set. In this paper, we propose an interference cancellation method that models the interference as a (possibly large) number of sinusoidal interference signals, being present in both the primary and secondary data. This form of interference occurs in a variety of applications, such as, for instance, nuclear quadrupole resonance (NQR) spectroscopy, where the primary data contains the signal signature of interest, corrupted by narrow-band interference signals, often being several magnitudes stronger than the SOI [14]. As the SOI decays rapidly, this allows for the possibility of measuring a secondary data set prior to the next excitation [5, 10]. Due to the relative stationarity of the typical interference signals, the described interference model will apply to the two data sets. Earlier work on interference cancellation in NQR spectroscopy has focused on forming projectors orthogonal to the subspace spanned by the interference [5, 10, 11], or on spaces close to the subspace formed from the dominant components in the secondary data [13]. These techniques offer notable interference rejection capabilities, except in cases when the interference occurs close to the frequencies of the SOI, which will, for instance, happen when using an excitation coil with a high Q-factor. In particular, for substances having few spectral lines, the performance degradation may in such cases be substantial. The here proposed interference rejection technique is instead constructed such that each dominant frequency component occurring in both the primary and the secondary data sets are removed, taking into account the unknown phase offset of each such component. We illustrate the performance of the proposed technique using both realistic simulation data as well as real NQR measurements, comparing to the earlier used techniques. This paper is organized as follows: In the next section, we outline the data model for the primary and secondary data sets and define the interference model. In Section 3, the proposed algorithm is derived, and in Section 4 numerical examples are presented. Finally, we conclude on the work in Section 5.

## 2. DATA MODEL

Consider the primary data set,

$$y_p(t) = s_p(t) + r_p(t) + e_p(t) \quad (1)$$

---

This work was supported in part by the Swedish Research Council, the European research council (ERC, Grant agreement n. 261670), STINT, and Carl Trygger's foundation.

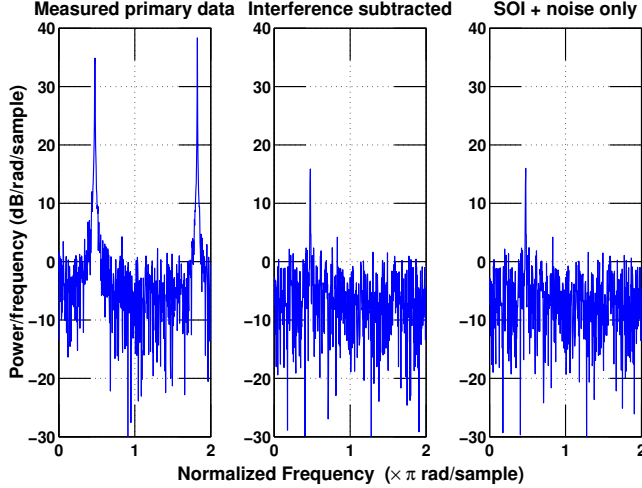


**Fig. 1.** Simulated NQR-signal with interference containing two sinusoids, one of which is on top of the NQR-signal and one which is randomly positioned. The left figure shows the measured primary data, whereas the middle figure shows the primary data after EPIC has removed the interference. The right figure shows the simulated NQR-signal without interference.

where  $s_p(t)$  denotes the SOI,  $r_p(t)$  the interference,  $e_p(t)$  the unstructured noise, often assumed to be a white Gaussian noise, and where  $t = t_0^p, t_1^p, \dots, t_{N_p}^p$  denotes the time instances for the primary data measurements. Similar, let the secondary data be formed as

$$y_s(t) = r_s(t) + e_s(t) \quad (2)$$

where  $t = t_0^s, t_1^s, \dots, t_{N_s-1}^s$  denote the measurement times of the secondary data set. We will herein consider two particular cases, namely when  $t_0^p = t_0^s$ , which corresponds to measuring the secondary data at the same time as the primary data, which, for instance, occurs in stochastic NQR (sNQR) measurements [5], as well as the case when  $t_{N_p-1}^p < t_0^s$ , for which the secondary data set is recorded at a time after the primary data set, such as is the case for, e.g., (conventional) NQR measurements [10]. These two situations, which are later discussed, have impact on the proposed method. Furthermore, the interference is modeled as

$$r(t) = \sum_{k=1}^K \alpha_k e^{2i\pi f_k t} \quad (3)$$

where  $\alpha_k = |\alpha_k|e^{-2i\pi\phi_k}$  denotes the complex amplitude, where  $\phi_k$  denotes the phase,  $f_k$  denote the frequency, and the subscript  $k$  denotes the  $k$ :th sinusoidal component in the interference. The number of interference components,  $K$ , is usually unknown and will here be treated as such. For the second

---

### Algorithm 1 EPIC

---

- 1: Given  $y_p$  and  $y_s$
  - 2: **while** (8) is not satisfied **do**
  - 3: Estimate the most dominant sinusoidal component in  $r_s$  using (5)
  - 4: Remove the found component from  $y_p$  using (6)
  - 5: Remove the found component from  $y_s$  using (7)
  - 6: **end while**
- 

case mentioned above, we have to assume that the interference is reasonably stationary and narrow-banded, whereas in the first case, this assumption can be somewhat relaxed and one may allow for interference containing also damped sinusoidal components.

### 3. PROPOSED METHOD

In the proposed method, we begin by determining the most dominant spectral components in the secondary data by minimizing (where in the first iteration  $k = 1$ )

$$\mathcal{C} = \min_{\alpha_k, f_k} \|\mathbf{y}_s^{k-1} - \alpha_k \mathbf{a}_k\|_2^2 \quad (4)$$

$$= \min_{f_k} \|\mathbf{y}_s^{k-1} - (\mathbf{a}_k^* \mathbf{a}_k)^{-1} \mathbf{a}_k^* \mathbf{y}_s^{k-1}\|_2^2 \quad (5)$$

typically by evaluating the cost function,  $\mathcal{C}$ , over a grid of frequencies, where  $\mathbf{y}_s^{k-1}$  denotes the vector containing the secondary data at iteration  $k$ ,  $\mathbf{a}_k = [e^{2i\pi f_k t_0}, \dots, e^{2i\pi f_k t_{N-1}}]^T$ , with  $(\cdot)^T$  denoting the transpose, is the Fourier vector for frequency  $f_k$ , and, where in (5),  $\alpha_k$  has been replaced by its least squares estimate. Then, the resulting spectral line may be subtracted from both the primary and secondary data sets. Clearly, the subtraction is highly sensitive to errors in the estimated phase,  $\phi = \angle \alpha$ . To allow for a better estimate, the frequency grid is preferably refined based on the previous estimate from (5), which then becomes the center of a new, finer, frequency grid on which a new minimization is made using (5). This is repeated until satisfactory resolution is reached and the estimates  $\hat{f}_k$ ,  $\hat{\phi}_k$ , and  $|\hat{\alpha}_k|$  may be determined with high precision. The estimated sinusoid is then subtracted from the primary data using

$$y_p^{(k)}(t) = y_p^{(k-1)}(t) - |\hat{\alpha}_k| e^{-2i\pi\hat{\phi}_k} e^{2i\pi\hat{f}_k t} \quad (6)$$

with  $t = t_0^p, t_1^p, \dots, t_{N_p}^p$ , whereas for the secondary data set

$$y_s^{(k)}(t) = y_s^{(k-1)}(t) - |\hat{\alpha}_k| e^{-2i\pi\hat{\phi}_k} e^{2i\pi\hat{f}_k t} \quad (7)$$

with  $t = t_0^s, t_1^s, \dots, t_{N_s-1}^s$ , where, for the both sets,  $k$  denotes the  $k$ :th interference component to be removed. This procedure is then repeated until the interference is deemed canceled. Since the number of interference components,  $K$ , is unknown, it is necessary to introduce some

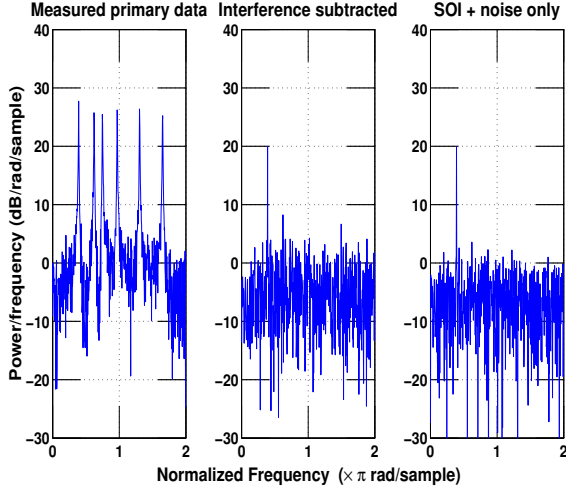


**Fig. 2.** Simulated NQR-signal with interference containing six damped sinusoids, randomly positioned. The left figure shows the measured primary data, whereas the middle figure shows the primary data after EPIC has removed the interference. The right figure shows the simulated NQR-signal without interference.

form of stopping criteria in the iteration. Here, we terminate the subtraction loop when

$$\|\mathbf{y}_s^{k-1} - \mathbf{y}_s^k\|_2 / \|\mathbf{y}_s^{k-1}\|_2 < \gamma \quad (8)$$

where  $\gamma$  is an appropriately selected user parameter. In our experience, the algorithm is not overly sensitive to the value of  $\gamma$ , but it will affect computation time. Empirically, we have found that a reasonable value is  $\gamma = 0.1$ . Setting  $\gamma$  too high, the probability of missing small interferences is increased, whereas if setting it too low, the algorithm starts to subtract noise, which does not impact noticeably on the result, but will increase the computation time. The proposed method, here termed EPIC (Estimation of Phase and amplitude for Interference Cancellation), is outlined in Algorithm 1, where  $\mathbf{y}_p$  is the vector containing the primary data, and  $\mathbf{r}_s$  is the vector containing the interference present in the secondary data set.

#### 4. NUMERICAL RESULTS

We initially examine a simulated sNQR signal [5], satisfying the above mentioned case 1, wherein the SOI, mimicking the NQR response of the narcotic methamphetamine, having only a single spectral line at 1.217 MHz, is corrupted by two strong narrow-banded interference signals, one of which coincides in frequency with the NQR signal, whereas the other is randomly positioned in the spectra. Figure 1 shows a typical example with the acquired primary data (left), the resulting data after applying EPIC (middle), and the simulated signal without interference (right). As is clear from the figure, EPIC

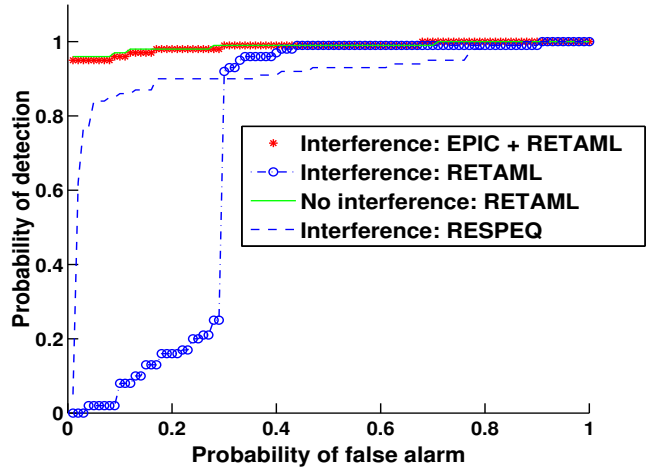


**Fig. 3.** ROC curves showing the performance of the proposed method as compared to the RESPEQ and RETAML algorithms, with  $SIR = -30$  dB and  $SNR = -15$  dB.

noticeably reduces the interference components, almost to the point where it is completely removed. Since the primary and secondary data sets are acquired simultaneously, the length of the two data sets are here selected to be the same, with  $N_p = N_s = 512$ . The user parameter is throughout the study set to  $\gamma = 0.1$ . A more complicated case is when the interference is made up by damped sinusoids. In this case, each of the damped components may then be approximated as a set of sinusoidal signals, such that

$$\alpha e^{(2i\pi f - \beta)t} \approx \sum_k \alpha_k e^{2i\pi f_k t} \quad (9)$$

where the range of frequencies  $\{f_k\}$  forms the support of  $e^{(2i\pi f - \beta)t}$ . Figure 2 illustrates the performance of the algorithm when the above noted interference is replaced by six damped sinusoids components, clearly showing the efficiency of the EPIC algorithm also in this case. We proceed to examine a signal instead formed to mimic a conventional NQR signal of methamphetamine, satisfying case 2 above. The interference is made up by three large sinusoids, two of which are randomly distributed over the spectra, whereas one is randomly distributed within a small interval ( $\pm 16.7$  kHz) of the signal's signature peak. Figure 3 illustrates the ROC curves for the detection of the substance using the RETAML algorithm [5], with and without using the proposed EPIC interference cancellation, as compared with the RESPEQ algorithm [11], which uses a subspace-based interference rejection prior to forming the detection variable. As can be seen in the figure, the EPIC algorithm successfully cancels the interference, yielding almost the same performance as if the interference had not been present, whereas the RESPEQ algorithm notably suffers from the closely located interference compo-

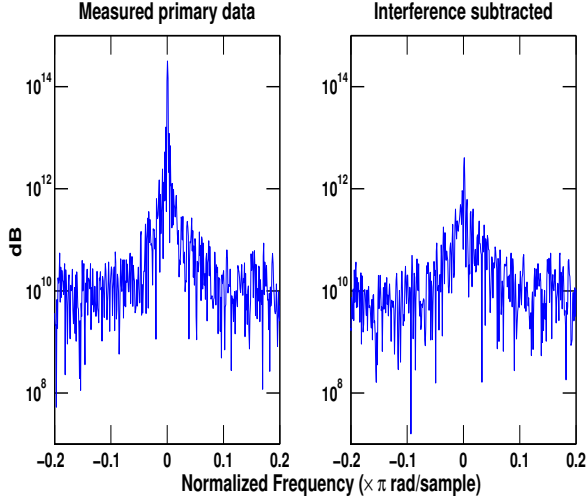


**Fig. 4.** Real NQR data where a sinusoidal interference is positioned on top of the NQR signal. The left figure shows the measured primary data whereas the right figure shows the primary data after removing the interference using the proposed algorithm.

ment. In these simulations,  $N_p = 512$  and  $N_s = 7\,680$ , with a signal to interference ratio (SIR) and the signal to noise ratio (SNR), defined as

$$\text{SIR} = 10 \log_{10} \left( \frac{P_{\text{signal}}}{P_{\text{interference}}} \right) \quad (10)$$

$$\text{SNR} = 10 \log_{10} \left( \frac{P_{\text{signal}}}{P_{\text{noise}}} \right) \quad (11)$$

where  $P_{\text{interference}}$  and  $P_{\text{noise}}$  denotes the average power of the interference and the noise, respectively, being set to  $\text{SIR} = -30$  dB and  $\text{SNR} = -15$  dB. As a final example, we examine measured NQR data. In this case, we examine the NQR response of imidazole, having a single spectral peak at 1.369 MHz. In these measurements, two cases are examined; one where a strong interference component is present at the same frequency as the SOI, whereas in the other case the interference is instead close, but not on, the SOI. Figures 4 and 5 show the results for the two cases. In the experiments, the secondary data, containing  $N_s = 4\,000$  samples, was collected just after the primary data, which contained  $N_p = 1\,000$  samples, with the interference being created by an oscillator which was set at the frequency 1.369 MHz for the first case, and at 1.371 MHz in the second case. The secondary data was measured when the NQR pulsing was stopped, thereby only measuring the background noise and the interference. We note that, when doing NQR-measurements, it is common to set the excitation frequency at, or close to, the same frequency as the received NQR-signal, which is the explanation as to why, after demodulation, the peak appears at frequency zero. As can be seen from the figures, the interference is suc-

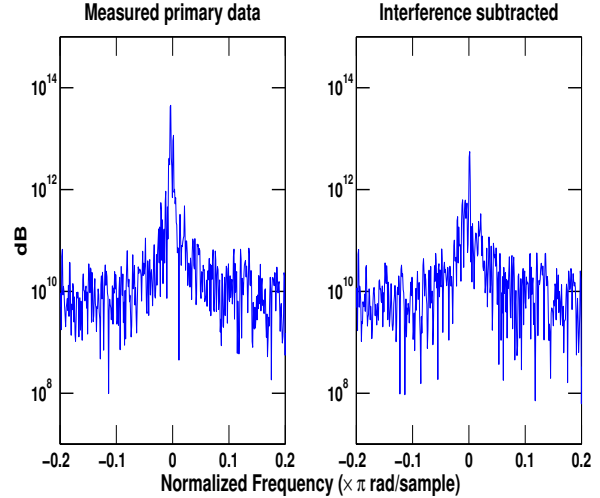


**Fig. 5.** Real NQR data where a sinusoidal interference is positioned very close to the NQR signal. The left figure shows the measured primary data whereas the right figure shows the primary data after removing the interference using the proposed algorithm.

cessfully removed in both cases, showing the resulting undisturbed NQR-signal.

## 5. CONCLUSION

In this paper, we have presented a novel interference cancellation method exploiting a secondary data set to reduce the influence of interference components occurring in both the primary and secondary data sets. In contrast to existing techniques, the algorithm is able to handle also cases when the interference components are overlapping the signal of interest. Numerical examples using both simulated and measured spectroscopic data illustrates the preferable performance of the proposed method as compared to recent state-of-the-art cancellation algorithms.

## 6. ACKNOWLEDGMENT

The authors would like to thank Professor Hideo Itozaki and Associate Professor Hideo Sato-Akaba at Osaka University, Japan, for valuable discussions and for providing the NQR data used in this paper.

## REFERENCES

- [1] P. Stoica, H. He, and J. Li, "Optimization of the Receive Filter and Transmit Sequence for Active Sensing," *IEEE Transactions on Signal Processing*, vol. 60, pp. 1730–1740, april 2012.

- [2] F. Bandiera, A. De Maio, A. S. Greco, and G. Ricci, "Adaptive Radar Detection of Distributed Targets in Homogeneous and Partially Homogeneous Noise Plus Subspace Interference," *IEEE Transactions on Signal Processing*, vol. 55, pp. 1223–1237, April 2007.
- [3] J. D. Laster and J. Reed, "Interference rejection in digital wireless communications," *IEEE Signal Processing Magazine*, vol. 14, pp. 37–62, May 1997.
- [4] J. G. Andrews, "Interference cancellation for cellular systems: a contemporary overview," *IEEE Wireless Communications*, vol. 12, pp. 19–29, April 2005.
- [5] S. D. Somasundaram, A. Jakobsson, M. D. Rowe, J. A. S. Smith, N. R. Butt, and K. Althoefer, "Robust Detection of Stochastic Nuclear Quadrupole Resonance Signals," *IEEE Transactions on Signal Processing*, vol. 56, pp. 4221–4229, September 2008.
- [6] N. R. Butt, E. Gudmundson, and A. Jakobsson, *An Overview of NQR Signal Detection Algorithms*. Springer, 2014. to appear.
- [7] D. Qu, Z. Wang, T. Jiang, and M. Daneshmand, "Side-lobe suppression using extended active interference cancellation with self-interference constraint for cognitive OFDM system," *Communications and Networking in China, 2009. ChinaCOM 2009. Fourth International Conference on*, pp. 1–5, 2009.
- [8] Z. Wang, S. Zhou, J. Catipovic, and P. Willett, "Back to Results Parameterized Cancellation of Partial-Band Partial-Block-Duration Interference for Underwater Acoustic OFDM," *IEEE Transactions on Signal Processing*, vol. 60, pp. 1782–1795, April 2012.
- [9] N. B. Pulsone and C. M. Rader, "Adaptive Beamformer Orthogonal Rejection Test," *IEEE Transactions on Signal Processing*, vol. 49, pp. 521–529, March 2001.
- [10] S. D. Somasundaram, A. Jakobsson, and N. R. Butt, "Countering Radio Frequency Interference in Single-Sensor Quadrupole Resonance," *IEEE Geoscience and Remote Sensing Letters*, vol. 6, pp. 62–66, Jan. 2009.
- [11] T. Rudberg and A. Jakobsson, "Robust Detection of Nuclear Quadrupole Resonance Signals in a Non-Shielded Environment," in *Proceedings of the 19th European Signal Processing Conference (EUSIPCO)*, 2011.
- [12] R. T. Behrens and L. L. Scharf, "Signal Processing Applications of Oblique Projection Operators," *IEEE Transactions on Signal Processing*, vol. 42, pp. 1413–1424, June 1994.
- [13] A. Svensson and A. Jakobsson, "Adaptive Detection of a Partly Known Signal Corrupted by Strong Interference," *IEEE Signal Processing Letters*, vol. 18, pp. 729–732, Dec. 2011.
- [14] S. D. Somasundaram, A. Jakobsson, J. A. S. Smith, and K. Althoefer, "Exploiting Spin Echo Decay in the Detection of Nuclear Quadrupole Resonance Signals," *IEEE Transactions on Geoscience and Remote Sensing*, vol. 45, pp. 925–933, April 2007.